
Biomarkers

ISSN: 1354-750X (Print) 1366-5804 (Online) Journal homepage: www.tandfonline.com/journals/ibmk20

# Placenta specific 1: a novel marker for detection of metastasis in mouse model of breast cancer

Sadegh Safaei, Masoumeh Dehghan Manshadi, Hannaneh Golshahi, Farideh Hashemi, Farhang Sasani, Zahra Madjd & Roya Ghods

**To cite this article:** Sadegh Safaei, Masoumeh Dehghan Manshadi, Hannaneh Golshahi, Farideh Hashemi, Farhang Sasani, Zahra Madjd & Roya Ghods (10 Sep 2025): Placenta specific 1: a novel marker for detection of metastasis in mouse model of breast cancer, Biomarkers, DOI: 10.1080/1354750X.2025.2556166

**To link to this article:** https://doi.org/10.1080/1354750X.2025.2556166

View supplementary material

Published online: 10 Sep 2025.

Submit your article to this journal

Article views: 61

View related articles

View Crossmark data

Full Terms & Conditions of access and use can be found at
https://www.tandfonline.com/action/journalInformation?journalCode=ibmk20

BIOMARKERS
https://doi.org/10.1080/1354750X.2025.2556166

Taylor & Francis
Taylor & Francis Group

Check for updates

RESEARCH ARTICLE

# Placenta specific 1: a novel marker for detection of metastasis in mouse model of breast cancer

Sadegh Safaei[a,b,c*], Masoumeh Dehghan Manshadi[a,b*#], Hannaneh Golshahi[d], Farideh Hashemi[a,b], Farhang Sasani[e], Zahra Madjd[a,b] and Roya Ghods[a,b]

[a]Oncopathology Research Center, Iran University of Medical Sciences, Tehran, Iran; [b]Department of Molecular Medicine, Faculty of Advanced Technologies in Medicine, Iran University of Medical Sciences, Tehran, Iran; [c]Monoclonal Antibody Research Center, Avicenna Research Institute, ACECR, Tehran, Iran; [d]Nanobiotechnology Research Center, Avicenna Research Institute, ACECR, Tehran, Iran; [e]Department of Pathology, Faculty of Veterinary Medicine, University of Tehran, Tehran, Iran

**ABSTRACT**

**Background:** Placental-specific 1 (Plac1), with no expression in normal tissues, is expressed in different cancers. Therefore, the potential application of Plac1 to detect metastasis was investigated in breast cancer model.

**Methods:** A spontaneous metastasis model was established using 4T1 cells. FDG-PET and histological analysis were used to detect metastasis. Plac1 expression was assessed in a wide range of tumor-bearing and normal mice tissues by RT-qPCR. The sensitivity of Plac1-positive cell detection was examined by 4T1 serial dilution in Plac1-negative cells.

**Results:** Plac1 was not expressed in normal mouse tissues (n=6), except in the brain (6/6, dCT=−10.85). 4T1 cell line (dCT=0.65) and 4T1-induced tumor (dCT=−0.29) were positive for Plac1 expression. PET imaging and histopathology analysis demonstrated metastases in the lung, liver, and spleen of tumor-bearing mice. Plac1 expression was confirmed in lung (6/6, dCT=−1.52), liver (6/6, dCT=−2.37), spleen (6/6, dCT=−3.7), kidney (2/6, dCT=−40.00), brain (6/6, dCT=−7.47), and blood (6/6, dCT=−3.35) of tumor-bearing mice. The sensitivity of detecting tumor cells is at least one cell per million cells.

**Conclusions:** Plac1 is a novel marker with high specificity and sensitivity for detecting metastasis in breast cancer. These findings provide a rationale for human studies.

Abbreviation: TNBC: Triple Negative Breast Cancer; Plac1: Mouse Placental-specific 1; PLAC1: Human Placental-specific 1; Gapdh: Mouse glyceraldehyde-3-phosphate dehydrogenase; GAPDH: Human glyceraldehyde-3-phosphate dehydrogenase; PBMC: Peripheral Blood Mononuclear Cell; PET: Positron Emission Tomography; $^{18}$F-FDG: $^{18}$-Fluorodeoxyglucose; NBF: Neutral Buffered Formalin; H&E: Hematoxylin and Eosin; MI: Mitotic Index; HPF: High Power Fields

**ARTICLE HISTORY**
Received 20 December 2024
Accepted 30 August 2025

**KEYWORDS**
Metastasis detection; Disseminated tumor cells; Biomarker; Placenta-specific 1; Breast cancer; 4T1 cell line

## Introduction

Despite significant improvements in the detection of metastasis as the main cause of cancer-related mortality, identification of disseminated tumor cells or metastasis remains a challenge (Ganesh and Massagué 2021; Sauer et al. 2021). There are several approaches for metastasis detection in animal models and humans. The most common methods are biopsy evaluation of involved organs, radiological assessments, and imaging techniques (Menezes et al. 2016). In spite of the fact that these methods have reduced the rate of cancer-related mortality associated with metastasis, they are frequently incapable of detecting metastasis at the earliest stage and accurately predicting the clinical prognosis of the disease (Scully et al. 2012).

The utilization of diagnostic biomarkers can improve the accuracy and specificity of metastasis identification. An ideal tumor marker should have remarkable sensitivity, specificity, and reliability, which can be beneficial in detecting metastasis, detecting recurrent disease, and monitoring therapy response (Malati 2007). In general, a critical factor in evaluating a biomarker's diagnostic value for metastasis detection, regardless of the sample type (blood, urine, tissue, etc.) and the measurement procedure, is its specificity and sensitivity. For example, current serum biomarkers used for metastasis detection, including CK19, CEA, CA15-3, MUC1, mammaglobin, maspin, VEGF, and TGF-b, have several limitations (Schoenfeld et al. 1994; Amoils et al. 1996; Luppi et al. 1996; Min et al. 1998; Gillanders et al. 2004; Zhang et al. 2021; Tarighati et al. 2023). Many of these biomarkers have insufficient sensitivity for detecting micro metastases, which can result in missed diagnoses and delayed treatment (Malati 2007). These markers are often expressed in both cancerous

CONTACT Roya Ghods ghods.ro@iums.ac.ir, rghods77@yahoo.com; Zahra Madjd majdjabari.z@iums.ac.ir, zahra.madjd@yahoo.com Oncopathology Research Center, Iran University of Medical Sciences, Tehran, Iran.
*Sadegh Safaei and Masoumeh Dehghan Manshadi contributed equally to this manuscript as co-first authors
#Masoumeh Dehghan Manshadi is responsible for statistical design and analysis. Email: masoumehdehghan60@gmail.com
Supplemental data for this article can be accessed online at https://doi.org/10.1080/1354750X.2025.2556166.
© 2025 Informa UK Limited, trading as Taylor & Francis Group

and normal tissues, which leads to reduced specificity and an increased likelihood of false positives, particularly in patients with non-cancerous conditions (Luo et al. 2022; Passaro et al. 2024; Zhou et al. 2024). Therefore, a critical factor in evaluating a biomarker is its specific expression in cancer cells and absence in normal physiological conditions.

Placenta-specific protein 1 (PLAC1) is an X-linked cancer-testis antigen with no detectable expression in normal tissues except testis, placenta, and cerebellum (Fant et al. 2002; Massabbal et al. 2005; Koslowski et al. 2007; Silva et al. 2007; Wang et al. 2014). Ectopic expression of PLAC1 has been reported in a wide variety of tumors, including breast, prostate, liver, lung, stomach, ovary, colon, head and neck, and pancreas (Mahmoudian et al. 2019). Several studies have shown PLAC1 expression in a variety of cancer cell lines originating from different tumors (Silva et al. 2007). The physiological role of this molecule appears to be essential for normal development of placenta, which includes trophoblast cell migration (Muto et al. 2016; Mahmoudian et al. 2019). The oncogenic function of PLAC1 has been revealed in several studies. The silencing of PLAC1 in breast cancer cells led to a decrease in proliferation, an increase in apoptosis, and a significant impairment in cell migration and invasion (Koslowski et al. 2007; Meng et al. 2022). As a promising candidate for metastasis diagnostic marker, PLAC1 has received considerable attention in recent years (Ma et al. 2021; Meng et al. 2022). Overall, these data suggest that PLAC1 could be an attractive candidate among tumor-specific genes for the identification of disseminated tumor cells and metastasis.

In order to develop and validate a new diagnostic candidate for metastasis detection or treatment response monitoring, several animal models have been established (Gómez-Cuadrado et al. 2017). Animal models provide a controlled and repeatable setting that could be used to investigate the complex biological processes involved in cancer metastasis. The spontaneous breast cancer metastasis model using 4T1 is widely used to mimic metastatic breast cancer (Tao et al. 2008). In this model, 4T1 metastasizes to several distant organs, including lung, liver, brain, and bone, and closely resembles human breast cancer metastasis (Pulaski and Ostrand-Rosenberg 2001; Tao et al. 2008). This model is particularly useful for biomarker recognition, validation, and assessment of response to therapy (Anisiewicz et al. 2018; Lu et al. 2022).

In this study, for the first time, we evaluated Plac1 as a marker for mouse breast cancer metastasis detection. For this purpose, metastatic breast cancer mouse model was established, and the presence of metastasis was assessed via Positron Emission Tomography (PET) scan, histopathology, and also validated by Plac1 mRNA expression using real-time PCR. Our findings regarding the identification of cancer cells using Plac1 as a sensitive marker provide a basis for further investigations in humans. Notably, 82% of human breast tumors express PLAC1 molecule (Koslowski et al. 2007), suggesting that the current findings will likely be confirmed in human studies. These findings highlight the potential utility of PLAC1 for metastasis detection, particularly when used in immunoPET imaging protocols that target tumor-specific antigens. The results of our study may lead to the introduction of a novel diagnostic marker for detecting and monitoring metastasis in breast cancer patients.

## Materials and methods

### *Cancer cell line culture*

Mouse breast cancer cell line 4T1 (Plac1-positive) and human colorectal cancer cell line HT-29 (Plac1-negative) were obtained from the National Cell Bank of Iran (Pasteur Institute of Iran, Tehran, Iran) and the Iranian Biological Resource Center (IBRC, Tehran, Iran), respectively. 4T1 cells were cultured in RPMI-1640 medium (Sigma, Germany), and HT-29 cells were cultured in Dulbecco's Modified Eagle medium (DMEM)/High glucose medium (Gibco, Germany), supplemented with 10% heat-inactivated fetal bovine serum (FBS) (Gibco, Germany) and 1% penicillin/streptomycin (Biowest, France). Cell lines were cultured at 37°C in a humidified atmosphere (95%) containing 5% CO2. The cells were passaged when cell confluency reached 80%.

### *Animal model of spontaneous breast cancer metastasis*

All animal experiments were performed according to the committee's ethical guidelines for animal laboratories at Iran University of Medical Sciences (IUMS) (Ethics Committee Number: IR.IUMS.AEC.1402.066). Six-week-old female Balb/c mice were purchased from Royan Institute of Iran (Tehran, Iran). All of the standard care was provided for the mice: food, water, a light/dark cycle, an appropriate temperature, and humidity. The mice were kept for one-week adaptation period in the laboratory environment prior to being subjected to experiments. Mice were divided into two groups: tumor-induced group ($n=6$) and normal group ($n=6$).

For tumor induction, 4T1 cells were dissociated using 0.05% trypsin/EDTA (Gibco, Germany) and resuspended in complete media. Single cells were washed twice with cold phosphate- buffered saline (PBS). For tumor induction, $1 \times 10^5$ 4T1 cells in 0.1 ml of PBS were subcutaneously injected into the right mammary fat pad of mice. Tumor growth was measured every two days using digital calipers after palpation.

### *PET scan studies*

PET imaging has been widely used as a diagnostic tool in clinical practice to assess the location(s) of metastasis (Almuhaideb et al. 2011). Detection of metastasis was evaluated in tumor-bearing mice using $^{18}$F-fluorodeoxyglucose (FDG) PET scans when the primary tumors attained a maximum dimension of approximately 1.8 centimeters, as well as in normal mice for comparative purposes. Notably, two randomly selected mice from each group (tumor-bearing and normal groups) underwent both PET imaging and subsequent histopathological examination to ensure unbiased sampling and representative analysis. All mice were fasted for 10 hours prior to PET imaging tests. Mice were weighed and anesthetized using 2% isoflurane mixed with oxygen before tail vein injection of $^{18}$F-FDG. The injected dose of $^{18}$F-FDG was calculated using a dose calibrator (300 μCi). The PET scan was started 60 minutes post-injection to allow optimal $^{18}$F-FDG distribution and tissue uptake. Subsequently, each mouse underwent a 10-minute PET scan to ensure adequate data acquisition for high-quality images reconstruction. PET scan was performed using a small-animal multi-modality scanner (Xtrim-PET Scanner, PNP Co., Iran). A detailed description of the Xtrim-PET system has been reported elsewhere (Zeraatkar et al. 2017; Amirrashedi et al. 2019). The system has a spatial resolution of 2.1 mm. The PET data were reconstructed using a $256 \times 256 \times 47$ matrix size to balance spatial resolution and noise reduction. Whole body images were acquired with 2 bed positions for a mouse. The images were reconstructed and analyzed using image reconstruction software (XtrimVision) and VivoQuant software. For the quantitative analysis of PET images, tumor-to-background ratio (TBR) and organ-to-background ratio (OBR) were calculated. TBR and OBR are established methods for quantifying the uptake of the imaging agent $^{18}$F-FDG in tumor tissues relative to normal organs and their respective background signals. This approach has been extensively validated in various cancer models, including breast cancer (Rezaei Aghdam et al. 2022; Shirke et al. 2024). In this study, background signal intensity was determined by averaging three distinct regions of interest (ROIs) that were confirmed to be unaffected by metastasis. For the calculation of TBR and OBR, three-dimensional regions of interest (ROIs) were meticulously delineated around the tumor, lung, liver, and spleen. The TBR and OBR values were derived from the ROIs using the following formula: (ROI counts per voxel)/(background counts per voxel) (Rezaei Aghdam et al. 2022; Barzegar Behrooz et al. 2024). After PET imaging ($30 \pm 3.36$ days after tumor cells injection), all mice were sacrificed by CO2 asphyxiation, and primary tumors, liver, lung, brain, kidney, spleen, and blood were harvested.

## Histological analysis

Tumors and organs of interest were fixed in 10% neutral buffered formalin (NBF). Tissues were processed and embedded in paraffin, and then 5 µm sections were prepared for hematoxylin and eosin (H&E) staining. The slides were screened for tumor metastases by board-certified veterinary pathologists (H.G. & F.S.).

## RNA isolation and quantitative real-time PCR (RT-qPCR)

To assess Plac1 expression, total RNAs were extracted from 4T1 and HT29 cell lines, 4T1-tumor, blood, whole lung, liver, spleen, kidney, and brain tissues in both groups of mice (tumor-bearing and normal) using the One Step-RNA Reagent (Bio Basic, Canada) according to the manufacturer's instructions. In addition, RNA was extracted from mouse testis as a positive tissue control for Plac1 expression. RNA quantity and integrity were assessed by Nanodrop (ThermoFisher Scientific, USA) and gel electrophoresis. To eliminate possible genomic DNA contamination, RNA samples were treated with DNase I. RNA was reverse transcribed into cDNA using the cDNA Synthesis Kit (Yekta Tajhiz Azma, YT4500, Iran). Real-time PCR was performed with the PCR Master Mix Green-High Rox A325402-25 (Ampliqon, Denmark) by the RotorGene Q LightCycler (Qiagene, Germany). The expression of glyceraldehyde-3-phosphate dehydrogenase (mouse Gapdh and human GAPDH) was considered as internal control for 4T1 and HT29, respectively. PCR reactions were carried out in the following steps: 95°C for 10 minutes, 45 cycles of amplification (denaturation at 95°C for 15 seconds, annealing at 60°C for 15 seconds, and extension at 72°C for 15 seconds), and final melt curve analysis performed in the range of 65°C to 95°C to exclude non-specific PCR products. RT-qPCR data were analyzed using the comparative Ct (Cycle threshold) method to present relative expression levels of the genes. The Plac1 primers were designed, and the specificity of the primer sequences was evaluated using the Primer-BLAST tool on the NCBI website. The primers designed in this study exhibit specificity for the mouse Plac1 and do not detect human PLAC1. The primer sequences are listed in Table 1.

## Determination of RT-qPCR sensitivity for detection of Plac1-positive cells

In the sensitivity test, Plac1-positive cells were mixed with negative cells (the primers are specifically designed to amplify only the murine target molecule). This approach has been widely employed in previous studies (Schneider et al. 2002; Havens et al. 2008; Alcoser et al. 2011). To measure the sensitivity of RT-qPCR assays to detect Plac1-positive cells, 4T1 cells (Plac1-positive) were serially mixed with HT29 cells (Plac1-negative) to obtain the dilution range between $10^2$ and $10^6$ (one 4T1 in $10^2$ to $10^6$ HT29) (Stutterheim et al. 2008; Dahn et al. 2021). The minimum dilution level at which the average ΔCt value was at least 3.0 Ct lower than the average ΔCt of the negative cell was determined as sensitivity (Anisiewicz et al. 2018). Therefore, sensitivity was defined as the lowest dilution at which Plac1 detected.

## Statistical analysis

Statistical analysis was performed with GraphPad Prism version 8.0 for Windows (GraphPad Software, La Jolla, CA, USA, www.graphpad.com). Expression of Plac1 mRNA was tested with the RT-qPCR and calculated with Pfaffl's rule (Pfaffl 2001; Pfaffl et al. 2002; Vandesompele et al. 2002). The relative and normalized expression ratio is calculated based on the median and IQR. Statistical significance was accepted at p-values ≥0.05.

Table 1. Primers used for real-time PCR.

| Gene | Forward primer (5′-3′) | Reverse primer (5′-3′) | Product size (bp) |
|---|---|---|---|
| Mouse Gapdh | AACTTTGGCATTGTGGAAGG | CACATTGGGGGTAGGAACAC | 222 |
| Human GAPDH | CATGAGAAGTATGACAACAGCCT | AGTCCTTCCACGATACCAAAGT | 113 |
| Mouse Plac1 | AGGAGAATCCTTCCTGGACG | GTCGAGCACAGCACATTCAC | 157 |

## Results

Herein, we detected metastasis in 4T1-tumor model by $^{18}$FDG-PET and histological analysis and consequently validated and compared these methods with RT-qPCR to detect Plac1-positive tumor cells in mouse tissues. We summarized the study design and findings in Figure 1.

### *Validation of metastasis by $^{18}$FDG-PET*

Following the implantation of 4T1 cells into the mammary fat pad of Balb/c mice, on average, on the ninth day after injection, the tumors became palpable in all mice. Every two days measurements of tumor dimension using a digital caliper revealed that 4T1 tumors reached 18 mm in the largest dimension 30 ± 3.36 days after tumor cells injection. At this stage, PET scan was performed using glucose analog PET radiotracer $^{18}$F-FDG for detection of 4T1 metastasis lesions. In addition, PET scans were done in normal mice to compare the images of two groups of mice. As expected, analysis of images showed $^{18}$F-FDG uptake in the 4T1 primary tumor in mammary of the female Balb/c mice. Also, PET images showed increased FDG uptake in the lung and liver of tumor-bearing mice, indicating the existence of metastatic lesions in these organs. Moreover, signal was detected in spleen of tumor-bearing mice, and splenomegaly was also observed in this group. No signal was detected in corresponding tissues in normal mice. In both groups of mice (tumor-bearing and normal mice), signals were observed in brain and bladder due to high uptake of glucose in brain and accumulation of fluid in bladder (Almuhaideb et al. 2011; Zhu et al. 2011) (Figure 2). For quantitative analysis, we assessed $^{18}$F-FDG distribution in tumor, lung, liver, and spleen tissues of 4T1 tumor-bearing and normal mice by measuring TBR and OBR. In 4T1 tumor-bearing mice, TBR for the tumor and OBR for the lung, liver, and spleen were 4.5, 3.22, 3.39, and 6.1, respectively, measured at 60 minutes after injection. Also, in normal mice, TBR of corresponding tissue and OBR of lung, liver, and spleen were 1.63, 1.25, 1.49, and 1.48, respectively (Table 2). High OBR in the lung, liver, and spleen of tumor- bearing mice indicates the metastasis and presence of tumor cells.

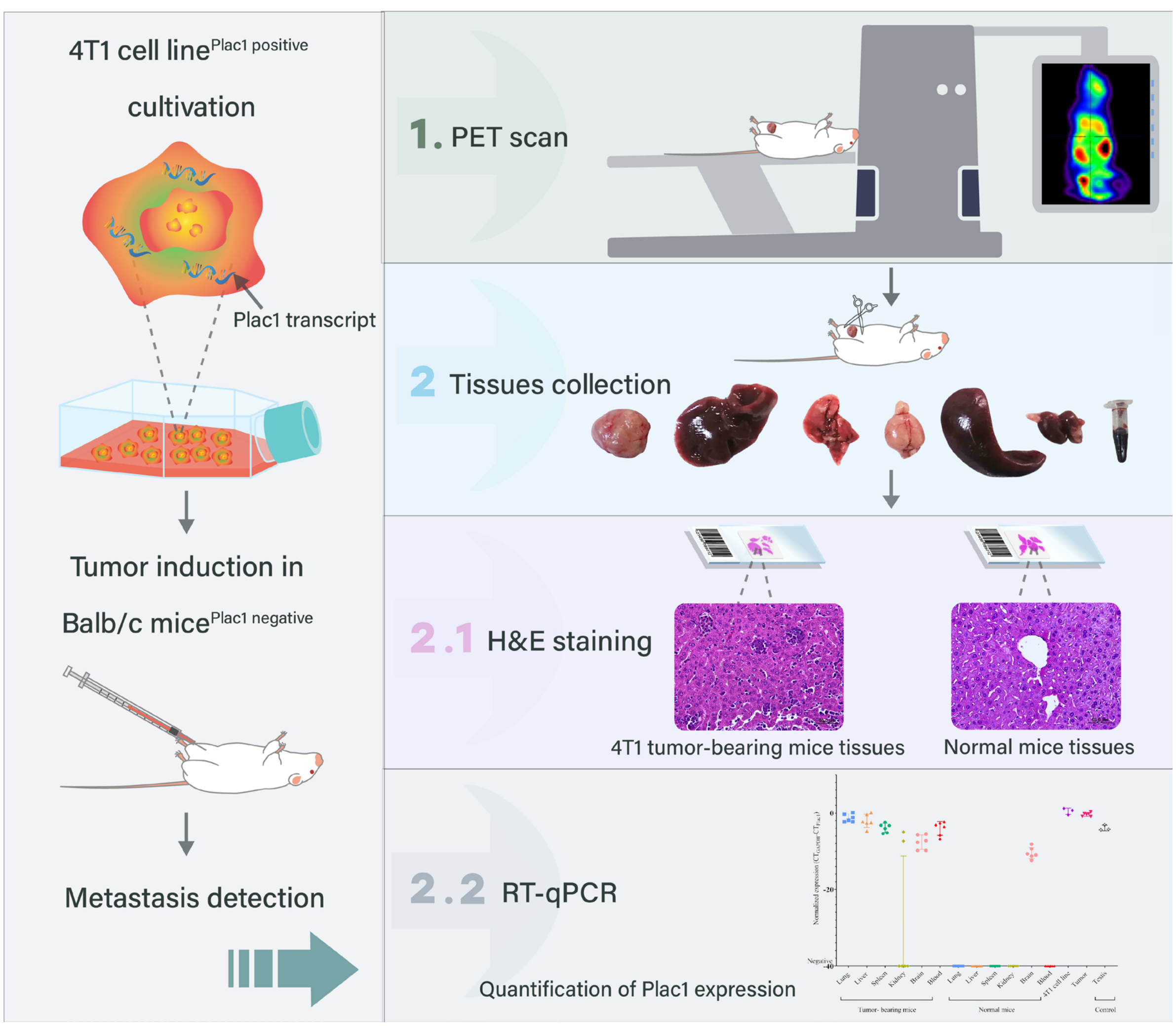


Figure 1. An overview of the study. A spontaneous metastasis model of breast cancer was constructed using injection of 4T1 cell line into mice mammary fat pads. FDG-PET scanning was used to detect metastatic lesions. Following that, mice were sacrificed, and tumors, liver, lung, brain, kidney, spleen, and blood tissues were collected for histological analysis. Plac1 expression was assessed, compared, and validated in metastasis tissues using real-time quantitative PCR.

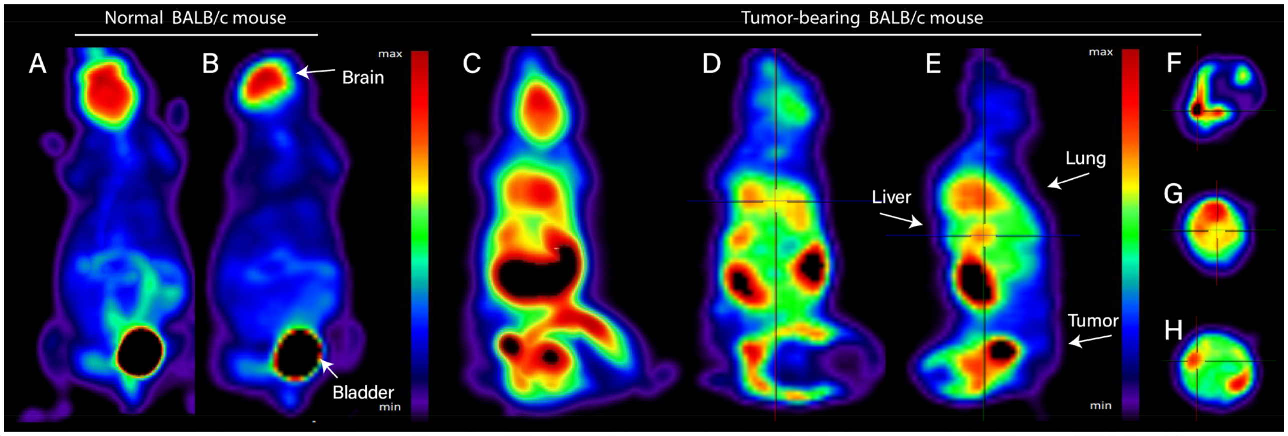


Figure 2. $^{18}$F-FDG PET scans of normal and 4T1 tumor-bearing female Balb/c mice. (A & B): normal mice, (A): Whole-body, (B): coronal view, FDG uptake was observed in brain and bladder. (C-H): 4T1 tumor-bearing female Balb/c mice. (C): Whole-body, (D): coronal view of PET image, (E): sagittal view that shows significant FDG uptake in tumor, lung, liver (white arrows), and spleen, (F): transverse plane of tumor (G): transverse plane of lung (H): transverse plane of liver.

Table 2. TBR and OBR values measured via PET scan in tumor-bearing and normal mice.

| Mouse model | TBR (tumor to background uptake ratio) | OBR (organ to background uptake ratio) | | |
|---|---|---|---|---|
| | | Lung | Liver | Spleen |
| **4T1 tumor-bearing mice** | 4.5 | 3.22 | 3.39 | 6.1 |
| **Normal mice** | 1.63 | 1.25 | 1.49 | 1.48 |

TBR = (number of counts in tumors per voxel)/(number of counts in background per voxel).
OBR = (number of counts in organs per voxel)/(number of counts in background per voxel).

### Histological analysis

Histopathological evaluation of 4T1 primary tumor revealed that the tumor consisted of sheaths of ovoid to round cells with poorly defined cytoplasm and vesiculated nuclei with prominent nucleoli. The mitotic index (MI) was 4–5/high power fields (HPF). There were some foci of necrosis within the tumor. In tumor bearing mice group, in lung and liver, multiple metastatic foci were observed. Metastatic foci consisted of round to oval-shaped tumor cells with scant cytoplasm. These cells had large hyperchromatic or large vesicular nuclei and single prominent nucleoli. Another pathological finding was interstitial granulocytic infiltration in pulmonary tissue, with no evidence of alveolar involvement. In hepatic tissue, noticeable number of granulocytes were seen in sinusoids and perivascular areas. In spleen, several small metastatic lesions, formation of extramedullary hematopoietic foci, reduction of white pulp area, and an increase in red pulp were also detected. In renal tissues, diffuse infiltration of acute inflammatory cells was seen in medullary zone. Furthermore, a notable infiltration of neutrophils in vasculatures in brain parenchyma was distinguished. In normal group, no pathological alterations were detected in all examined tissues (Figure 3).

### Quantification of mouse Plac1 expression

The level of Plac1 expression was assessed in mouse testis as a positive control, 4T1 and HT29 cell lines, 4T1 tumors, whole lung, liver, kidney, and brain, as well as the blood, via RT-PCR. Gapdh and GAPDH transcripts were used as internal controls for mouse samples (4T1 cells and mouse tissues) and HT29 cell line, respectively. The Ct expression values were used to calculate the median dCt for each sample ($dCT = CT_{Gapdh} - CT_{Marker}$). Any detectable expression of Plac1 was interpreted as a positive result. Plac1 expression was observed in the testis (dCT = −4.3 (−4.44 to −3.1)) as a Plac1-positive tissue. No amplification was detected when cDNA of HT29 cell line and Plac1 primers were used. Therefore, HT29 cell line was considered as the negative control for Plac1 amplification in this study. Expression of Plac1 was not observed in any examined organs of normal female mice except brain (6/6, dCT = −10.85 (−11.85 to −10.05)) after 45 cycles of PCR amplification.

Plac1 expression was demonstrated in the 4T1 cell line and the 4T1- induced tumor (4T1, dCT = 0.65 (−0.5 to 1.15) and tumor, dCT = −0.29 (−0.92 to −0.17)). Then, Plac1 expression as a representative of 4T1 was investigated in the mice tissues, including target tissues of breast cancer metastasis and other organs. The result showed that Plac1 was expressed in lung (6/6, dCT = −1.52 (−2.18 to −0.52)), liver (6/6, dCT = −2.37 (−2.57 to −0.86)), spleen (6/6, dCT = −3.7 (−4.92 to −3.26)), kidney (2/6, dCT = −40.00 (−40.0 to −5.67)), brain (6/6, dCT = −7.47 (−9.80 to −6.47)), and blood (6/6, dCT = −3.35 (−6.25 to −2.85)) of tumor-bearing mice (Table 2 and Figure 4). The expression levels of Plac1 in the lung, liver, spleen, brain, and blood were significantly different between the tumor-bearing and normal mice groups. The p-values are shown in Table 3. In addition, we observed higher dCT values in metastatic lung tissue compared to metastatic liver tissue; nonetheless, this difference was not statistically significant ($P = 0.38$).

### Sensitivity

The sensitivity of detection of Plac1 expression as a representative of 4T1 cells was evaluated using serial dilution mixtures of mouse 4T1 cells with human colorectal cancer cell line, HT29, as a negative cell for mouse Plac1 amplification ($10^{-1}$ to $10^{-6}$). While the HT29 cells showed no positive signal, as few as one 4T1 cell in one million human cells was detected (Table 4). Additionally, the correlation of 4T1 dilution factor with Ct values was evaluated. The strong

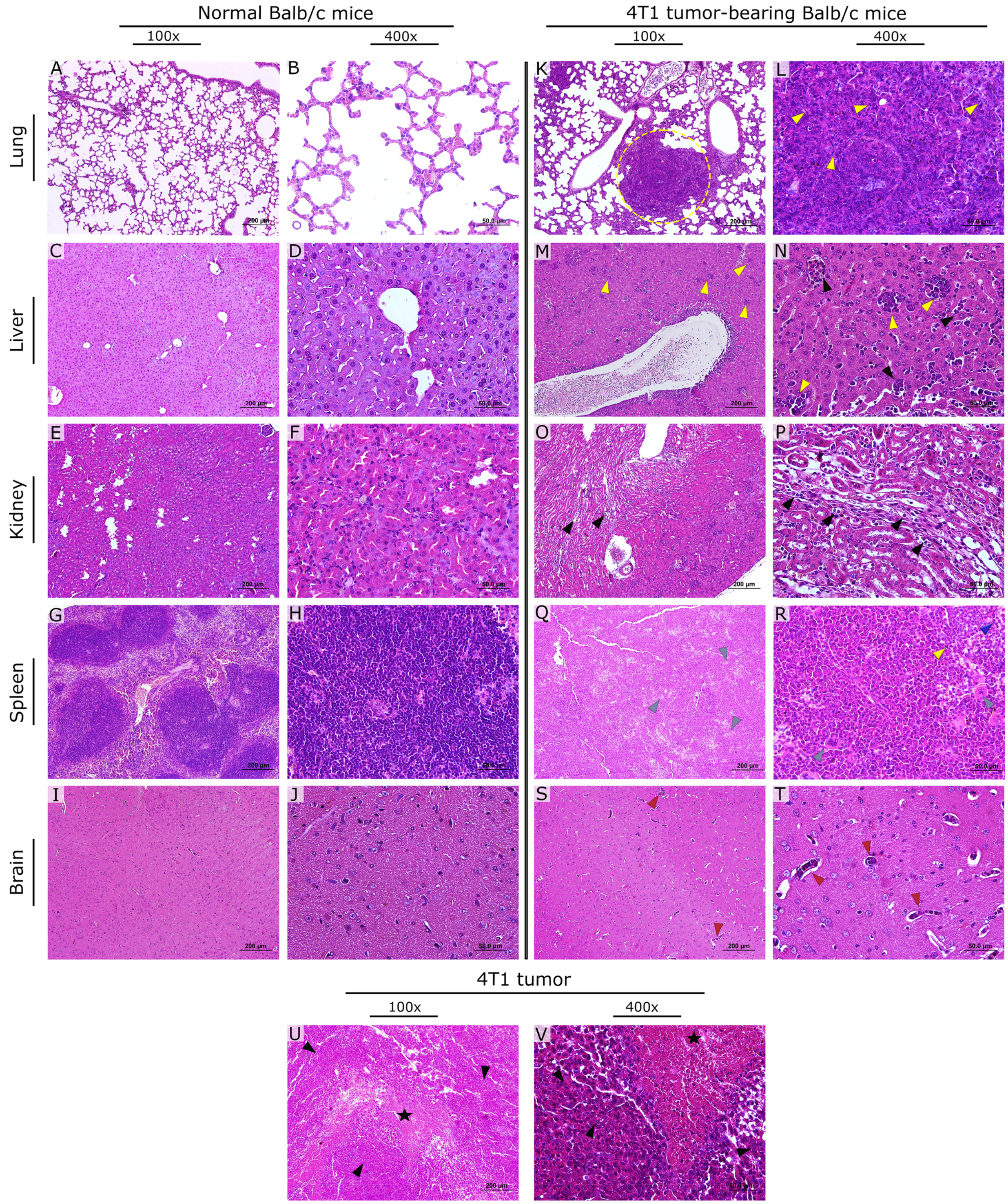


**Figure 3.** Representative images of H&E-stained sections of normal and 4T1 tumor-bearing female Balb/c mice tissues. (A-J): normal mice: no pathological alterations were detected. (A & B): lung, (C & D): liver, (E & F): kidney, (G & H): spleen, (I & J): brain. (K-T): 4T1 tumor-bearing female Balb/c mice, (K-L): lung; metastatic foci (yellow circle) and mitotic cells (yellow arrowhead) were observed in the lungs. (M-N): liver; metastatic foci were shown in the parenchyma (yellow arrowhead). Also, extensive acute inflammatory cell infiltration within the dilated hepatic sinusoids (black arrowhead) is seen. (O-P): kidney; the diffuse infiltration of inflammatory cells (black arrowhead) in the medullary zone was observed. (Q-R): spleen; metastatic cell (yellow arrowhead), hematopoietic cells (silver arrowhead), inflammatory cells (lymphocyte, blue arrowhead), and a significant reduction in white pulp and an increase in the red pulp area were observed (silver arrowhead). (S-T): brain; a significant infiltration of neutrophils (red arrowhead) in vasculatures was observed in brain parenchyma. (U-V): 4T1 tumors; solid patterns of irregularly rounded to spindle-shaped tumor cells with scant cytoplasm (black arrow) and necrotic foci (star) were observed (scale bar: A, C, E, G, I, K, M, O, Q, S, U: 200 µm, B, D, F, H, J, L, N, P, R, T, V: 50 µm).

correlation coefficient ($R2 = 0.9984$) indicates a reliable linear relationship between Log10(dilution factor) and mean Ct values (Supplementary Figure 1). It should be noted that the expression of GAPDH, a human housekeeping gene, was assessed via RT-qPCR to validate the efficiency of RNA extraction and cDNA synthesis in HT29 cells.

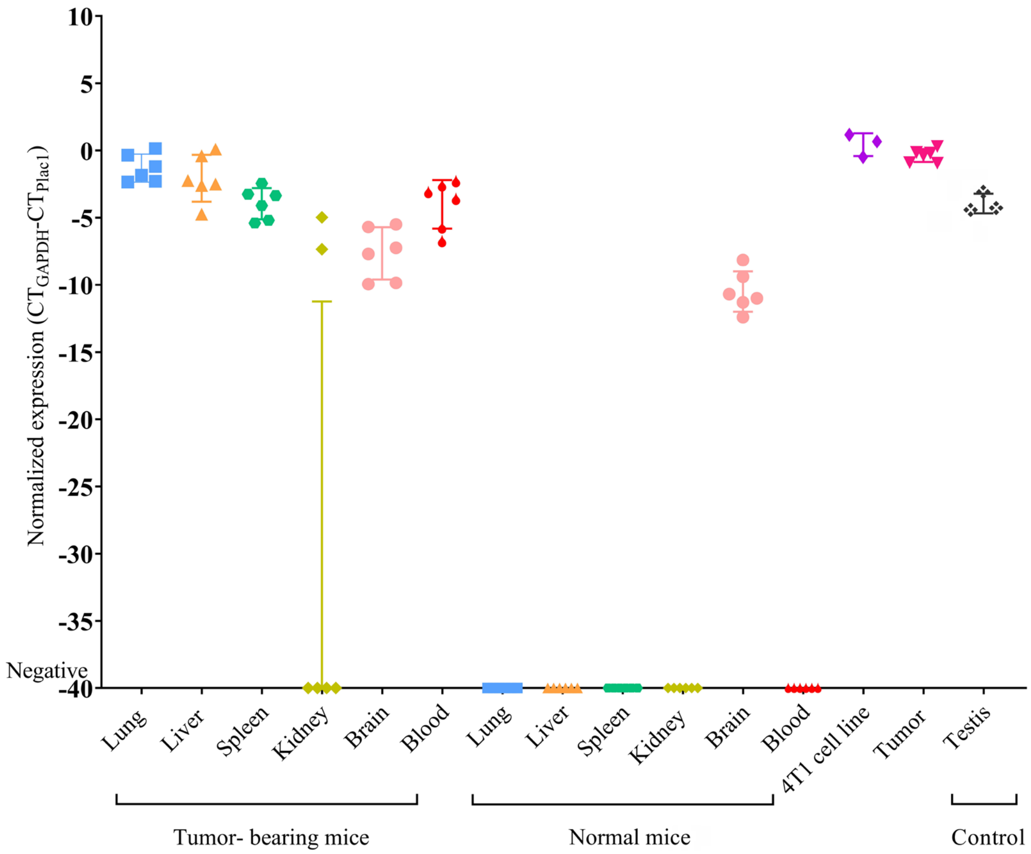


**Figure 4.** Normalized *Plac1* expression in different tissues of 4T1 tumor-bearing ($n=6$) and normal ($n=6$) mice. Plac1 expression was observed in the testis (dCT = −4.3 (−4.44 to −3.1)) as a Plac1-positive tissue and in the 4T1 cell line (dCT = 0.65 (−0.5 to 1.15)) and 4T1-induced tumor (dCT = −0.29 (−0.92 to −0.17)). In tumor-bearing mice, Plac1 was expressed in the lung (6/6, dCT = −1.52 (−2.18 to −0.52)), liver (6/6, dCT = −2.37 (−2.57 to −0.86)), spleen (6/6, dCT = −3.7 (−4.92 to −3.26)), kidney (2/6, dCT = −40.00 (−40.0 to −5.67)), brain (6/6, dCT = −7.47 (−9.80 to −6.47)), and blood (6/6, dCT = −3.35 (−6.25 to −2.85)). Expression of Plac1 was not observed in any examined organs of female control group except brain (6/6, dCT = −10.85 (−11.85 to −10.05)).

**Table 3.** Summary of metastasis detection in a spontaneous metastasis of breast cancer mouse model using PET imaging, histological analysis, and Plac1expression as a 4T1 representative marker.

| Method / Tissue | RT-qPCR: 4T1 tumor-bearing mice (n = 6) | | Normal mice (n = 6) | | | | PET scan | | Histological analysis | |
|---|---|---|---|---|---|---|---|---|---|---|
| | *Plac1* expression | **dCT**[a] median (IQR[c]) | *Plac1* expression | **dCT**[a] median (IQR) | *P-value* | Effect size | 4T1 tumor-bearing mice | Normal mice | 4T1 tumor-bearing mice | Normal mice |
| **Lung** | 6/6 | −1.52 (−2.18 to −0.52) | 0/6 | No amp[b] | **0.002** | **14.95** | Positive | Negative | Positive | Negative |
| **Liver** | 6/6 | −2.37 (−2.57 to −0.86) | 0/6 | No amp | **0.001** | **14.4** | Positive | Negative | Positive | Negative |
| **Spleen** | 6/6 | −3.7 (−4.92 to −3.26) | 0/6 | No amp | **0.002** | **12.275** | Positive | Negative | Positive | Negative |
| **Kidney** | 2/6 | −40.00 (−40.0 to −5.67) | 0/6 | No amp | 0.441 | **−1.6** | Negative | Negative | Negative | Negative |
| **Brain** | 6/6 | −7.47 (−9.80 to −6.47) | 6/6 | −10.85 (−11.85 to −10.05) | **0.024** | **3.375** | Positive | Positive | Negative | Negative |
| **Blood** | 6/6 | −3.35 (−6.25 to −2.85) | 0/6 | No amp | **0.001** | **10.775** | – | – | – | – |
| **4T1 cell line** | – | 0.65 (−0.5 to 1.15) | | | | | | | | |
| **HT29 cell line** | – | No amp | | | | | | | | |
| **4T1-tumor** (n = 6) | 6/6 | −0.29 (−0.92 to −0.17) | | | | | | | | |
| **Testis**[d] (n = 3) | 3/3 | −4.3 (−4.44 to −3.1) | | | | | | | | |

[a]Median and interquartile range (IQR) of normalized Ct values ($CT_{GAPDH}$-$CT_{Marker}$) was presented.
[b]No amplification was detected after 45 cycles of PCR.
[c]Interquartile range (IQR).
[d]Mouse testis was used as a Plac1 positive tissue.

Table 4. Sensitivity test: *Plac1* expression in serial dilution mixtures of 4T1 cells with HT29 cells presented as Ct levels.

| Dilution factor | $Ct_1$ value | $Ct_2$ value[a] | Mean Ct[b] |
|---|---|---|---|
| **10–2** | 30.1 | 30.3 | 30.2 |
| **10–3** | 31.6 | 32.1 | 31.8 |
| **10–4** | 33.1 | 32.9 | 33.0 |
| **10–5** | 34.8 | 34.1 | 34.4 |
| **10–6** | 35.7 | 35.8 | 35.7 |

[a]Ct1 and Ct2: The average of three separate tubes in one experiment is reported.
[b]Mean Ct: mean of Ct1 and Ct2 was presented.

Table 5. Comparison of four common techniques used in the detection of metastasis.

| Technique | Advantages | Disadvantages |
|---|---|---|
| **Real-Time PCR** | Highly sensitive, quantitative | No spatial information |
| **Imaging Techniques** (CT, MRI, PET) | Non-invasive, whole-body assessment, detects macroscopic metastases | Limited resolution for micrometastases, radiation exposure (CT/PET) |
| **IHC** (Immunohistochemistry) | High specificity, visualizes tissue architecture, detects protein expression | Semi-quantitative, limited to fixed tissues, subjective interpretation |
| **Flow Cytometry** | Quantitative, multi-parameter analysis | Requires cell suspension |

## Discussion

Metastasis is the leading cause of cancer death, and while immense strides have been made in cancer diagnosis and treatment approaches, patients with metastasis have a poor prognosis (Gerstberger et al. 2023). To overcome this problem, it is necessary to improve both therapeutic approaches and diagnostic methods. Identifying metastatic lesions, especially in the early stages of metastasis colonization, could improve treatment options, enhance the prognosis and the patient's quality of life (Lu et al. 2009). There are several approaches for metastasis detection, including molecular, histological, and imaging techniques (Aukema et al. 2009; Almuhaideb et al. 2011; Nakarai et al. 2015). The brief descriptions of some common techniques are provided. Currently, one of the most sensitive imaging techniques for detecting metastasis is PET scan (Zhu et al. 2011), meanwhile, it has been reported that tumor-to-background signal ratio is insufficient to detect small lesions and micrometastasis in breast cancer (Belohlavek 2008) and sensitivity was 53% for primary lesions < 5 mm (Cermik et al. 2008). Furthermore, FDG absorption was increased in tumor-induced inflamed organs, which decreased the reliability of the $^{18}$F-FDG PET signals (Okuma et al. 2006). Histological analyses, the gold-standard method, are commonly used to detect metastasis. Histological examination assesses a limited section of the tissues, thus enhancing the probability of false negative results. In addition, at least 10 tumor cells must be present in the lesion to be detectable in histological analysis (Nielsen et al. 2001). Immunohistochemistry (IHC) is considered as a powerful diagnostic tool for distinguishing primary from secondary malignancies through the identification of tissue-specific antigens. This is especially important in the cases of unknown primary tumors (Selves et al. 2018). For example, GATA3 and mammaglobin are used to confirm breast cancer metastasis (El Hag et al. 2017; De Lara et al. 2018). This technique enhances diagnostic accuracy and guides therapeutic decisions.

Flow cytometry is an analytical tool that enables quantification and characterization of circulating tumor cells (CTCs) in biological fluids, offering valuable insights into metastatic progression (Lopresti et al. 2019). The application of flow cytometry in metastasis research extends to monitoring minimal residual disease (MRD) and evaluating the efficacy of therapeutic interventions (Acosta et al. 2016; Sahu et al. 2021). Despite its advantages, this approach presents several challenges, including variability in sample preparation and the requirement for rigorously validated markers panel, which underscore the need for meticulous optimization. RT-qPCR has emerged as a potent tool for metastatic cancer detection due to its high sensitivity, specificity, and ability to quantify low-abundance nucleic acids (Mostert et al. 2015). By targeting tumor-specific biomarkers, such as metastasis-associated genes, qPCR enables the early identification of micrometastasis and disseminated tumor cells (Inokuchi et al. 2003; Kubota et al. 2003). Table 5 presents a comparison of the respective advantages and disadvantages associated with these techniques.

The presence of most common markers in normal samples could increase the probability of false-positive results (Andergassen et al. 2013). Thus, metastasis detection needs more sensitive and specific markers. PLAC1, a cancer-testis antigen with ectopic expression in a wide variety of cancers and no expression in normal tissues, is a promising marker for detecting metastasis and also targeted immunotherapy (Silva et al. 2007). In this study, for the first time, we have investigated potential use of mouse Plac1 as a tracker for detection of tumor cells in spontaneous metastasis model of breast cancer and consequently validated and compared Plac1 expression using RT-qPCR with $^{18}$FDG-PET and histological analysis of H&E-stained slides.

In the beginning, it was shown that Plac1 is not expressed in most normal mouse tissues, with the exception of the brain. Then, we confirmed that 4T1 expresses Plac1 molecule, which is consistent with the findings of earlier studies (Mahmoudian et al. 2019). Subsequently, following the establishment of the spontaneous metastasis breast cancer model, metastasis lesions were identified using whole-body PET imaging and histopathological examination. Afterwards, we investigated the expression of Plac1, which represents 4T1 tumor cells, in mouse tissues. In order to classify the discussion, each organ was separately discussed.

### *Lung metastasis*

Lungs are the most common sites for metastasis in 4T1 mouse mammary cancer model (Pulaski and Ostrand-Rosenberg 2001; duPre' et al. 2008). PET scan revealed the presence of multifocal metastases within the pulmonary area. Furthermore, the histological report confirmed the existence of metastasized cells within the lung. In 4T1 tumor model, we confirmed Plac1 expression in lungs using RT-qPCR. In addition, the lungs have a higher expression of Plac1 than other candidate metastatic sites, which could be due to the presence of more 4T1 cells. Other studies have also shown that the lung metastasis burden is higher than the liver metastasis in 4T1 breast cancer model (Arroyo-Crespo et al. 2019; Liu et al. 2021).

### Liver metastasis

Liver metastasis is a consequence of 4T1 tumor induction (Pulaski and Ostrand-Rosenberg 2001; Rashid et al. 2021). The PET imaging showed significant FDG uptake, which indicates liver metastases. Also, histologic examination of the liver of 4T1 tumor bearing mice revealed metastatic foci in parenchyma and extensive acute inflammatory cell infiltration within the dilated hepatic sinusoids, which is consistent with the imaging and histopathological results of other researchers (Tao et al. 2008; Peixoto et al. 2015). We also detected Plac1 in the liver tissues of all tumor bearing mice. Interestingly, Wang et al. found that PLAC1 is expressed in liver metastatic cells from colorectal cancer (Wang et al. 2023). We found a correlation between levels of Plac1 expression and the rate of metastasis in liver and lung as judged by PET imaging and metastatic foci. It is important to note, although the metastatic rate of 4T1 tumors to the lung is higher, the observed background ratio (OBR) in the liver and lung of 4T1-bearing mice remains comparable. This phenomenon may be attributed to hepatic glucose metabolism, which elevates background activity in the liver. Given that the liver is the central organ for glucose homeostasis, exhibits high metabolic activity, and receives a dual blood supply, the use of $^{18}$F-FDG for PET imaging results in substantial physiological uptake. Consequently, this leads to an inherently elevated background signal in hepatic PET scans (Sarikaya et al. 2021).

### Metastasis in brain

PET imaging revealed increased $^{18}$FDG uptake in the brain of normal and tumor-bearing mice. These signals in normal brain are because of the high metabolic demand of brain, which consumes significant amounts of glucose (Almuhaideb et al. 2011; Zhu et al. 2011). Therefore, it could interfere with the detection of cancer cells in the brain (Zhu et al. 2011). Also, based on presented data and previous studies (Fant et al. 2010; Mahmoudian et al. 2019), Plac1 is expressed in normal brain of mice; therefore, it seems that Plac1 is not a suitable marker for identifying metastatic cells in the brain, although its expression level was elevated in the brains of tumor bearing mice compared to the brains of normal mice, probably due to the presence of 4T1 cells. While expression of Plac1 in normal brain tissues diminishes its utility as a biomarker for detecting brain metastasis, our findings highlight its potential value in identifying metastatic lesions in other organs, particularly in the lungs and liver.

### Metastasis in spleen

PET scan results indicate increased $^{18}$FDG uptake in spleen of tumor bearing mice, and splenomegaly was also seen in this group. Other researchers have also reported splenomegaly in 4T1 tumor bearing mice (DuPre' and Hunter 2007). Quantification of PET scan results showed that the spleen in tumor-bearing mice had the highest OBR value, which could be due to the presence of 4T1 cells and also inflammation in the spleen. It is reported that the presence of tumor-induced inflammation in the spleen could result in PET scan signal observation (Okuma et al. 2006; Roomi et al. 2014; Zhao et al. 2022). Histologic examination of the spleen of 4T1 tumor bearing mice revealed several metastatic lesions, extramedullary hematopoietic activity, and extensive inflammatory cells. In the 4T1 model, Roomi et al. showed the presence of small metastatic lesions in the spleen using histopathology analysis (Roomi et al. 2014), and Tao et al. reported the presence of tumor cells in the spleen using imaging techniques (Tao et al. 2008). We also detected Plac1 in the spleen tissues of all tumor bearing mice.

### Metastasis in kidney

Two out of 6 tumor-bearing mice showed the expression of Plac1 as a representative of 4T1 metastatic cells in the kidney, which is comparable to the results of Tao et al., who reported that one out of six 4T1 tumor- bearing mice had metastasis in the kidney (Tao et al. 2008). However, PET imaging and histopathological analysis did not show metastasis. This issue may be due to the insensitivity of PET scans to detect lesions smaller than 2.1 millimeters in size (Rezaei Aghdam et al. 2022) and the limited number of examined slides. Considering the high sensitivity of real time PCR, this concern could be justified. Therefore, if the number of tumor cells is low (less than detection limit of PET), no tumor cells are detected by PET imaging, but it seems that examination of tumor cell specific transcripts such as Plac1 allows detection of even small numbers of tumor cells.

### Blood metastasis

To detect CTCs or mRNA of Plac1, we assessed presence of Plac1 transcript in blood of 4T1 tumor- bearing mice. Our results clearly showed that Plac1 transcript is detectable exclusively in the blood of tumor-bearing mice and absent in normal mice, suggesting its potential utility as a diagnostic biomarker pending validation in human cancer patients. In a human study, Guo et al. detected PLAC1 transcript in blood of hepatocarcinoma (HCC) patients using RT-qPCR (Guo et al. 2017). Currently, the identification of CTCs in the blood of cancer patients is of great importance; for example, FDA-approved CellSearch system (Veridex) is used to isolate CTCs for monitoring treatment responses in metastatic patients (Riethdorf et al. 2007). The basis of CellSearch system is selection of EPCAM positive carcinoma cells (Kling 2012). Considering that EPCAM is an epithelial marker, it is possible that the expression of this marker decreases during the epithelial-to- mesenchymal (EMT) process in carcinoma cells (Kalluri and Weinberg 2009; Yu et al. 2013). Therefore, it is required to identify a novel marker that lacks these limitations. If the results presented here are confirmed in human studies, PLAC1 may be considered a suitable candidate for identifying CTCs in PLAC1 positive-tumors.

One of the most important parameters in detection system is sensitivity. As demonstrated in the Results section, the sensitivity analysis revealed that this method can detect a single Plac1-positive cell among one million negative cells. While we did not empirically assess the sensitivity of this test with respect to transcript copy number, theoretical calculations allow for an approximate estimation of detectable copies. These calculations were derived from the most diluted test (one Plac1-positive cell per million negative cells). From the 20 µl of RNA extracted from these cell populations (10 4T1 cells in 10 million HT29 cells), 1 µl was used for cDNA synthesis in a final reaction volume of 20 µL, and then 1 µL of cDNA was used in real-time PCR (1/20 of the total RNA was reverse-transcribed into cDNA, and a further 1/20 of the resulting cDNA was used for real-time PCR analysis. Assuming Plac1 transcripts are expressed at moderate-to-high levels (100–1000 copies per cell) (Subkhankulova et al. 2008), the assay detects 2.5–25 copies. Although the estimated copy number expression of Plac1 in 4T1 cells may not be entirely accurate and should be interpreted as an approximation.

In line with this study, Guo et al. assessed the sensitivity of RT-qPCR for detection of MAGE-A1 and SSX1 transcripts by mixing the QGY7703 human HCC cell line and normal PBMCs. The reported sensitivity is 10 tumor cells per $10^7$ PBMCs (Acosta et al. 2016). The sensitivity of this technique in detecting CTCs was approximately one hundred times greater than that of conventional RT-PCR (Guo et al. 2017). In addition, it has been reported that the RT-qPCR detected one PSA-producing cell diluted into 1 x $10^6$ blood mononuclear cells (Ghossein et al. 1995).

Due to the importance of detecting metastasis, especially in the early stages, extensive research has been done mainly using animal models. Part of these research introduce markers that are not intrinsically expressed by tumor cells, which may be due to the lack of a tumor-specific marker with the potential to distinguish tumor cells from normal cells. Based on this approach, reporter genes were widely used for detection of tumor cells in metastatic organs. Deng et al. used firefly luciferase (Luc) transfected B16 cells to detect metastatic tumor cells in mouse organs using imaging and qPCR methods and showed that qPCR is at least 10 times more sensitive compared to imaging (Deng et al. 2017). Basically, the use of reporter genes for monitoring cancer cells is associated with some limitations; for example, the labeling process may affect cell behavior and its characteristics, and also cells may modify the expression of the reporter gene. GAPDH transcript has also been used to identify tumor cells in xenograft studies (Dahn et al. 2021). However, in syngeneic mouse models, the use of exogenous markers is associated with some limitations. Therefore, it is important to identify a marker that is only expressed in tumor cells and not in most normal tissues. Although several markers have been introduced for detection of metastatic cells, most of these markers have low diagnostic value due to their expression in normal tissues (Gould et al. 1995; Malati 2007). The expression pattern of Plac1 has made it an attractive molecule for tracking tumor cells.

The use of a panel of biomarkers (two or more markers) for the detection of metastasis offers significant advantages over single-marker approaches, including improved diagnostic accuracy, sensitivity, and specificity (Lee et al. 2023). By combining multiple markers, the panel can capture the heterogeneity of metastatic disease, reducing the likelihood of false negatives or positives that may arise from relying on a single biomarker. Additionally, a multi-marker approach enhances the ability to detect metastasis at earlier stages, as different biomarkers may reflect distinct aspects of tumor biology, such as invasion, angiogenesis, or immune evasion. This comprehensive profiling also allows for better risk stratification and personalized monitoring, ultimately supporting more informed clinical decision-making and improved patient outcomes (Kang et al. 2022). Given the characteristics of this molecule and the findings of this study, the incorporation of Plac1 molecule in conjunction with established biomarkers may enhance the early and accurate detection of metastatic disease.

In addition, it is conceivable that immunoPET using anti-Plac1/PLAC1 antibodies would allow the identification of metastatic lesions. In line with this assumption, a study showed that HER2-targeted PET/CT was effective in detecting small HER2-positive lesions and assessing the real-time HER2 status in breast cancer patients (Gao et al. 2024).

All the data show that according to the characteristics of PLAC1 (lack of expression in normal tissues and its expression in a wide variety of tumor cells), this molecule could be a detector of tumor cells. If these findings are also shown in metastatic lesions of human breast cancer, immuno PET using anti-PLAC1 antibodies can probably pave the way to identify small metastatic lesions. It should be noted that Koslowski et al. have shown PLAC1 expression in 82% of primary breast cancers (Koslowski et al. 2007), and the PLAC1 expression was detected in metastatic cells (Wang et al. 2023). Therefore, this molecule could be used for metastatic detection and treatment response monitoring in PLAC1-positive cancer patients. Nevertheless, an important limitation of this study is that the utility of this molecule for metastasis detection remains to be validated in other preclinical breast cancer models.

## Conclusion

Our data suggest that Plac1 is a promising biomarker for metastasis detection in a cancer mouse model. If these results are confirmed in human studies, PLAC1 could be used as a marker for detecting metastatic lesions in PLAC1-positive breast cancer patients. ImmunoPET targeting the PLAC1 molecule with specific antibodies may improve the detection of metastatic lesions in breast cancer patients.

## Acknowledgment

This study was supported by a grant from Iran University of Medical Sciences (Grant Number: 1402-1-28-25877). Moreover, the authors would like to acknowledge Tehran University of Medical Sciences Preclinical Core Facility (TPCF) for performing the PET scan. The authors would like to thank Dr. Ali-Reza Attar Rezaei for carefully proofreading of the manuscript and Dr. Saeed Talebi for interpretation of RT-qPCR data.

## Ethical approval

All procedures in this study were conducted in accordance with protocols approved by the Research Ethics Committee of Iran University of Medical Sciences, Tehran, Iran (IR.IUMS.AEC.1402.066).

## Authors' contributions

Conceptualization: Roya Ghods, Sadegh Safaei; Methodology: Masoumeh Dehghan Manshadi and Sadegh Safaei; Pathology analysis: Hannaneh Golshahi and Farhang Sasanih; Formal analysis and investigation: Roya Ghods, Sadegh Safaei, and Masoumeh Dehghan Manshadi; Writing—original draft preparation: Roya Ghods, Sadegh Safaei, Masoumeh Dehghan Manshadi, and Farideh Hashemi; Project administration, supervision, validation, and editing: Roya Ghods and Zahra Madjd. All authors reviewed the manuscript.

## Disclosure statement

No potential conflict of interest was reported by the author(s).

## Funding

This work was supported by a grant from Iran University of Medical Sciences (Grant Number: 1402-1-28-25877).

## Data availability

The dataset used in this study are available from the corresponding author upon formal request.

## References

Acosta M, Pereira J, Arroz M. 2016. Screening of carcinoma metastasis by flow cytometry: a study of 238 cases. Cytometry B Clin Cytom. 90(3):289–294. doi: 10.1002/cyto.b.21258

Alcoser SY, Kimmel DJ, Borgel SD, Carter JP, Dougherty KM, Hollingshead MG. 2011. Real-time PCR-based assay to quantify the relative amount of human and mouse tissue present in tumor xenografts. BMC Biotechnol. 11(1):124. doi: 10.1186/1472-6750-11-124

Almuhaideb A, Papathanasiou N, Bomanji J. 2011. 18F-FDG PET/CT imaging in oncology. Ann Saudi Med. 31(1):3–13. doi: 10.4103/0256-4947.75771

Amirrashedi M, Sarkar S, Ghafarian P, Hashemi Shahraki R, Geramifar P, Zaidi H, Ay MR. 2019. NEMA NU-4 2008 performance evaluation of Xtrim-PET: a prototype SiPM-based preclinical scanner. Med Phys. 46(11):4816–4825. doi: 10.1002/mp.13785

Amoils K, Seymour L, Bezwoda W. 1996. Comparison between immunocytochemical and polymerase chain reaction techniques for detection of oestrogen receptor and transforming growth factor β in breast cancer. Br J Cancer. 73(10):1255–1259. doi: 10.1038/bjc.1996.240

Andergassen U, Kölbl AC, Hutter S, Friese K, Jeschke U. 2013. Detection of circulating tumour cells from blood of breast cancer patients via RT-qPCR. Cancers (Basel). 5(4):1212–1220. doi: 10.3390/cancers5041212

Anisiewicz A, Pawlik A, Filip-Psurska B, Turlej E, Dzimira S, Milczarek M, Gdesz K, Papiernik D, Jarosz J, Kłopotowska D, et al. 2018. Unfavorable effect of calcitriol and its low-calcemic analogs on metastasis of 4T1 mouse mammary gland cancer. Int J Oncol. 52(1):103–126. doi: 10.3892/ijo.2017.4185

Arroyo-Crespo JJ, Armiñán A, Charbonnier D, Deladriere C, Palomino-Schätzlein M, Lamas-Domingo R, Forteza J, Pineda-Lucena A, Vicent MJ. 2019. Characterization of triple-negative breast cancer preclinical models provides functional evidence of metastatic progression. Int J Cancer. 145(8):2267–2281. doi: 10.1002/ijc.32270

Aukema TS, Straver ME, Valdés Olmos RA, Vogel WV. 2009. A different role for FDG PET/CT in axillary lymph node staging in breast cancer. Eur J Nucl Med Mol Imaging. 36(11):1896–1897. doi: 10.1007/s00259-009-1211-0

Barzegar Behrooz A, Latifi-Navid H, Lotfi J, Khodagholi F, Shojaei S, Ghavami S, Fahanik Babaei J. 2024. CSF amino acid profiles in ICV-streptozotocin-induced sporadic Alzheimer's disease in male Wistar rat: a metabolomics and systems biology perspective. FEBS Open Bio. 14(7):1116–1132. doi: 10.1002/2211-5463.13814

Belohlavek O. 2008. What is the role of FDG-PET in the initial staging of breast cancer? Eur J Nucl Med Mol Imaging. 35(3):472–474. doi: 10.1007/s00259-007-0643-7

Cermik TF, Mavi A, Basu S, Alavi A. 2008. Impact of FDG PET on the preoperative staging of newly diagnosed breast cancer. Eur J Nucl Med Mol Imaging. 35(3):475–483. doi: 10.1007/s00259-007-0580-5

Dahn ML, Dean CA, Jo DB, Coyle KM, Marcato P. 2021. Human-specific GAPDH qRT-PCR is an accurate and sensitive method of xenograft metastasis quantification. Mol Ther Methods Clin Dev. 20:398–408. doi: 10.1016/j.omtm.2020.12.010

De Lara S, Parris TZ, Werner Rönnerman E, Helou K, Kovács A. 2018. GATA 3 as a putative marker of breast cancer metastasis—a retrospective immunohistochemical study. Breast J. 24(2):184–188. doi: 10.1111/tbj.12863

Deng W, McLaughlin SL, Klinke DJ. 2017. Quantifying spontaneous metastasis in a syngeneic mouse melanoma model using real time PCR. Analyst. 142(16):2945–2953. doi: 10.1039/c7an00623c

DuPre' SA, Hunter KW. 2007. Murine mammary carcinoma 4T1 induces a leukemoid reaction with splenomegaly: association with tumor-derived growth factors. Exp Mol Pathol. 82(1):12–24. doi: 10.1016/j.yexmp.2006.06.007

duPre' SA, Redelman D, Hunter KW. 2008. Microenvironment of the murine mammary carcinoma 4T1: endogenous IFN-γ affects tumor phenotype, growth, and metastasis. Exp Mol Pathol. 85(3):174–188. doi: 10.1016/j.yexmp.2008.05.002

El Hag MI, Hag AM, Ha JP, Michael CW. 2017. Comparison of GATA-3, mammaglobin, GCDFP-15 expression in breast carcinoma in serous effusions: a cell-block micro-array study. Pleura Peritoneum. 2(3):143–148. doi: 10.1515/pp-2017-0014

Fant M, Farina A, Nagaraja R, Schlessinger D. 2010. PLAC1 (Placenta-specific 1): a novel, X-linked gene with roles in reproductive and cancer biology. Prenat Diagn. 30(6):497–502. doi: 10.1002/pd.2506

Fant M, Weisoly DL, Cocchia M, Huber R, Khan S, Lunt T, Schlessinger D. 2002. PLAC1, a trophoblast-specific gene, is expressed throughout pregnancy in the human placenta and modulated by keratinocyte growth factor. Mol Reprod Dev. 63(4):430–436. doi: 10.1002/mrd.10200

Ganesh K, Massagué J. 2021. Targeting metastatic cancer. Nat Med. 27(1):34–44. doi: 10.1038/s41591-020-01195-4

Gao F, Liu F, Wang J, Bi J, Zhai L, Li D. 2024. Molecular probes targeting HER2 PET/CT and their application in advanced breast cancer. J Cancer Res Clin Oncol. 150(3):118. doi: 10.1007/s00432-023-05519-y

Gerstberger S, Jiang Q, Ganesh K. 2023. Metastasis. Cell. 186(8):1564–1579. doi: 10.1016/j.cell.2023.03.003

Ghossein RA, Scher HI, Gerald WL, Kelly W, Curley T, Amsterdam A, Zhang Z-F, Rosai J. 1995. Detection of circulating tumor cells in patients with localized and metastatic prostatic carcinoma: clinical implications. J Clin Oncol. 13(5):1195–1200. doi: 10.1200/JCO.1995.13.5.1195

Gillanders WE, Mikhitarian K, Hebert R, Mauldin PD, Palesch Y, Walters C, Urist MM, Mann GB, Doherty G, Herrmann VM, et al. 2004. Molecular detection of micrometastatic breast cancer in histopathology-negative axillary lymph nodes correlates with traditional predictors of prognosis: an interim analysis of a prospective multi-institutional cohort study. Ann Surg. 239(6):828–840. doi: 10.1097/01.sla.0000128687.59439.d6

Gómez-Cuadrado L, Tracey N, Ma R, Qian B, Brunton VG. 2017. Mouse models of metastasis: progress and prospects. Dis Model Mech. 10(9):1061–1074. doi: 10.1242/dmm.030403

Gould VE, Bloom KJ, Franke WW, Warren WH, Moll R. 1995. Increased numbers of cytokeratin-positive interstitial reticulum cells (CIRC) in reactive,

inflammatory and neoplastic lymphadenopathies: hyperplasia or induced expression? Virchows Arch. 425(6):617–629. doi: 10.1007/BF00199352
Guo L, Xu D, Lu Y, Peng J, Jiang L. 2017. Detection of circulating tumor cells by reverse transcription-quantitative polymerase chain reaction and magnetic activated cell sorting in the peripheral blood of patients with hepatocellular carcinoma. Mol Med Rep. 16(5):5894–5900. doi: 10.3892/mmr.2017.7372
Havens AM, Pedersen EA, Shiozawa Y, Ying C, Jung Y, Sun Y, Neeley C, Wang J, Mehra R, Keller ET, et al. 2008. An in vivo mouse model for human prostate cancer metastasis. Neoplasia. 10(4):371–380. doi: 10.1593/neo.08154
Inokuchi M, Ninomiya I, Tsugawa K, Terada I, Miwa K. 2003. Quantitative evaluation of metastases in axillary lymph nodes of breast cancer. Br J Cancer. 89(9):1750–1756. doi: 10.1038/sj.bjc.6601248
Kalluri R, Weinberg RA. 2009. The basics of epithelial-mesenchymal transition. J Clin Invest. 119(6):1420–1428. doi: 10.1172/JCI39104
Kang KN, Koh EY, Jang JY, Kim CW. 2022. Multiple biomarkers are more accurate than a combination of carbohydrate antigen 125 and human epididymis protein 4 for ovarian cancer screening. Obstet Gynecol Sci. 65(4):346–354. doi: 10.5468/ogs.22017
Kling J. 2012. Beyond counting tumor cells. Nat Biotechnol. 30(7):578–580. doi: 10.1038/nbt.2295
Koslowski M, Sahin U, Mitnacht-Kraus R, Seitz G, Huber C, Türeci O. 2007. A placenta-specific gene ectopically activated in many human cancers is essentially involved in malignant cell processes. Cancer Res. 67(19):9528–9534. doi: 10.1158/0008-5472.CAN-07-1350
Kubota K, Nakanishi H, Hiki N, Shimizu N, Tsuji E, Yamaguchi H, Mafune K, Tange T, Tatematsu M, Kaminishi M. 2003. Quantitative detection of micrometastases in the lymph nodes of gastric cancer patients with real-time RT-PCR: a comparative study with immunohistochemistry. Int J Cancer. 105(1):136–143. doi: 10.1002/ijc.11031
Lee D, Yoon W, Lee A, Han Y, Byun Y, Kang JS, Kim H, Kwon W, Suh Y, Choi Y, et al. 2023. Multi-biomarker panel prediction model for diagnosis of pancreatic cancer. J Hepato Biliary Pancreat. 30(1):122–132. doi: 10.1002/jhbp.986
Liu Y, Gargesha M, Qutaish M, Zhou Z, Qiao P, Lu Z-R, Wilson DL. 2021. Quantitative analysis of metastatic breast cancer in mice using deep learning on cryo-image data. Sci Rep. 11(1):17527. doi: 10.1038/s41598-021-96838-y
Lopresti A, Malergue F, Bertucci F, Liberatoscioli ML, Garnier S, DaCosta Q, Finetti P, Gilabert M, Raoul JL, Birnbaum D, et al. 2019. Sensitive and easy screening for circulating tumor cells by flow cytometry. JCI Insight. 5(14):e128180. doi: 10.1172/jci.insight.128180
Lu D, Zhou H, Li N, Wang Y, Zhang T, Wang F, Liu N, Zhu H, Zhang J, Yang Z, et al. 2022. Galectin expression detected by 68Ga-galectracer PET as a predictive biomarker of radiotherapy resistance. Eur J Nucl Med Mol Imaging. 49(8):2746–2760. doi: 10.1007/s00259-022-05711-1
Lu J, Steeg PS, Price JE, Krishnamurthy S, Mani SA, Reuben J, Cristofanilli M, Dontu G, Bidaut L, Valero V, et al. 2009. Breast cancer metastasis: challenges and opportunities. Cancer Res. 69(12):4951–4953. doi: 10.1158/0008-5472.CAN-09-0099
Luo J, Xiao J, Yang Y, Chen G, Hu D, Zeng J. 2022. Strategies for five tumour markers in the screening and diagnosis of female breast cancer. Front Oncol. 12:1055855. doi: 10.3389/fonc.2022.1055855
Luppi M, Morselli M, Bandieri E, Federico M, Marasca R, Barozzi P, Ferrari M, Savarino M, Frassoldati A, Torelli G. 1996. Sensitive detection of circulating breast cancer cells by reverse-transcriptase polymerase chain reaction of maspin gene. Ann Oncol. 7(6):619–624. doi: 10.1093/oxfordjournals.annonc.a010680
Ma J, Li L, Du J, Pan C, Zhang C, Chen Y. 2021. Placenta-specific protein 1 enhances liver metastatic potential and is associated with the PI3K/AKT/NF-κB signaling pathway in colorectal cancer. Eur J Cancer Prev. 30(3):220–231. doi: 10.1097/CEJ.0000000000000611
Mahmoudian J, Ghods R, Nazari M, Jeddi-Tehrani M, Ghahremani M, Ostad S, Zarnani A. 2019. Expression profiling of plac1 in murine cancer cell lines. Exp Oncol. 41(1):7–13. doi: 10.32471/exp-oncology.2312-8852.vol-41-no-1.12743
Mahmoudian J, Ghods R, Nazari M, Jeddi-Tehrani M, Ghahremani MH, Ghaffari-Tabrizi-Wizsy N, Ostad SN, Zarnani A-H. 2019. PLAC1: biology and potential application in cancer immunotherapy. Cancer Immunol Immunother. 68(7):1039–1058. doi: 10.1007/s00262-019-02350-8
Malati T. 2007. Tumour markers: an overview. Indian J Clin Biochem. 22(2):17–31. doi: 10.1007/BF02913308
Massabbal E, Parveen S, Weisoly D, Nelson DM, Smith S, Fant M. 2005. PLAC1 expression increases during trophoblast differentiation: evidence for regulatory interactions with the fibroblast growth factor-7 (FGF-7) axis. Mol Reprod Dev. 71(3):299–304. doi: 10.1002/mrd.20272
Menezes M, Das S, Minn I, Emdad L, Wang X-Y, Sarkar D, Pomper M, Fisher P. 2016. Detecting tumor metastases: the road to therapy starts here. Adv Cancer Res. 132:1–44. doi: 10.1016/bs.acr.2016.07.001
Meng X, Liu Z, Zhang L, He Y. 2022. Plac1 remodels the tumor immune evasion microenvironment and predicts therapeutic response in head and neck squamous cell carcinoma. Front Oncol. 12:919436. doi: 10.3389/fonc.2022.919436
Min CJ, Tafra L, Verbanac KM. 1998. Identification of superior markers for polymerase chain reaction detection of breast cancer metastases in sentinel lymph nodes. Cancer Res. 58(20):4581–4584.
Mostert B, Sieuwerts AM, Bolt-de Vries J, Kraan J, Lalmahomed Z, van Galen A, van der Spoel P, de Weerd V, Ramírez-Moreno R, Smid M, et al. 2015. mRNA expression profiles in circulating tumor cells of metastatic colorectal cancer patients. Mol Oncol. 9(4):920–932. doi: 10.1016/j.molonc.2015.01.001
Muto M, Fujihara Y, Tobita T, Kiyozumi D, Ikawa M. 2016. Lentiviral vector-mediated complementation restored fetal viability but not placental hyperplasia in Plac1-deficient mice. Biol Reprod. 94(1):6–19. doi: 10.1095/biolreprod.115.133454
Nakarai C, Osawa K, Akiyama M, Matsubara N, Ikeuchi H, Yamano T, Hirota S, Tomita N, Usami M, Kido Y. 2015. Expression of AKR1C3 and CNN3 as markers for detection of lymph node metastases in colorectal cancer. Clin Exp Med. 15(3):333–341. doi: 10.1007/s10238-014-0298-1
Nielsen BS, Lund LR, Christensen IJ, Johnsen M, Usher PA, Wulf-Andersen L, Frandsen TL, Danø K, Gundersen HJG. 2001. A precise and efficient stereological method for determining murine lung metastasis volumes. Am J Pathol. 158(6):1997–2003. doi: 10.1016/S0002-9440(10)64671-8
Okuma T, Matsuoka T, Okamura T, Wada Y, Yamamoto A, Oyama Y, Koyama K, Nakamura K, Watanabe Y, Inoue Y. 2006. 18F-FDG small-animal PET for monitoring the therapeutic effect of CT-guided radiofrequency ablation on implanted VX2 lung tumors in rabbits. J Nucl Med. 47(8):1351–1358.
Passaro A, Al Bakir M, Hamilton EG, Diehn M, André F, Roy-Chowdhuri S, Mountzios G, Wistuba II, Swanton C, Peters S. 2024. Cancer biomarkers: emerging trends and clinical implications for personalized treatment. Cell. 187(7):1617–1635. doi: 10.1016/j.cell.2024.02.041
Peixoto RCA, Miranda-Vilela AL, de Souza Filho J, Carneiro MLB, Oliveira RGS, da Silva MO, de Souza AR, Báo SN. 2015. Antitumor effect of free rhodium (II) citrate and rhodium (II) citrate-loaded maghemite nanoparticles on mice bearing breast cancer: a systemic toxicity assay. Tumour Biol. 36(5):3325–3336. doi: 10.1007/s13277-014-2966-x
Pfaffl MW, Horgan GW, Dempfle L. 2002. Relative expression software tool (REST©) for group-wise comparison and statistical analysis of relative expression results in real-time PCR. Nucleic Acids Res. 30(9):e36-e36–36. doi: 10.1093/nar/30.9.e36
Pfaffl MW. 2001. A new mathematical model for relative quantification in real-time RT–PCR. Nucleic Acids Res. 29(9):e45-e45–45. doi: 10.1093/nar/29.9.e45
Pulaski BA, Ostrand-Rosenberg S. 2001. Mouse 4T1 breast tumor model. Curr Protoc Immunol. 20(1):20.2. doi: 10.1002/0471142735.im2002s39
Rashid NS, Grible JM, Clevenger CV, Harrell JC. 2021. Breast cancer liver metastasis: current and future treatment approaches. Clin Exp Metastasis. 38(3):263–277. doi: 10.1007/s10585-021-10080-4
Rezaei Aghdam H, Bitarafan Rajabi A, Sadat Ebrahimi SE, Beiki D, Abdi K, Mousavi Motlagh SS, Kiani Dehkordi B, Darbandi Azar A, Shafiee Ardestani M. 2022. 18F-FDG MicroPET and MRI targeting breast cancer mouse model with designed synthesis nanoparticles. J Nanomater. 2022(1):5737835. doi: 10.1155/2022/5737835

Riethdorf S, Fritsche H, Müller V, Rau T, Schindlbeck C, Rack B, Janni W, Coith C, Beck K, Jänicke F, et al. 2007. Detection of circulating tumor cells in peripheral blood of patients with metastatic breast cancer: a validation study of the CellSearch system. Clin Cancer Res. 13(3):920–928. doi: 10.1158/1078-0432.CCR-06-1695

Roomi M, Kalinovsky T, Roomi N, Cha J, Rath M, Niedzwiecki A. 2014. In vitro and in vivo effects of a nutrient mixture on breast cancer progression. Int J Oncol. 44(6):1933–1944. doi: 10.3892/ijo.2014.2379

Sahu S, Gupta P, Susheilia S, Gautam U, Dey P. 2021. Application of multicolour flow cytometry in the detection of metastatic carcinoma in serous effusions: special emphasis in atypical cytology. Cytopathology. 32(2):169–179. doi: 10.1111/cyt.12922

Sarikaya I, Schierz J-H, Sarikaya A. 2021. Sarikaya A: liver: glucose metabolism and 18F-fluorodeoxyglucose PET findings in normal parenchyma and diseases. Am J Nucl Med Mol Imaging. 11(4):233–249.

Sauer S, Reed DR, Ihnat M, Hurst RE, Warshawsky D, Barkan D. 2021. Innovative approaches in the battle against cancer recurrence: novel strategies to combat dormant disseminated tumor cells. Front Oncol. 11:659963. doi: 10.3389/fonc.2021.659963

Schneider T, Osl F, Friess T, Stockinger H, Scheuer WV. 2002. Quantification of human Alu sequences by real-time PCR–an improved method to measure therapeutic efficacy of anti-metastatic drugs in human xenotransplants. Clin Exp Metastasis. 19(7):571–582. doi: 10.1023/a:1020992411420

Schoenfeld A, Luqmani Y, Smith D, O'reilly S, Shousha S, Sinnett H, Coombes R. 1994. Detection of breast cancer micrometastases in axillary lymph nodes by using polymerase chain reaction. Cancer Res. 54(11):2986–2990.

Scully OJ, Bay B-H, Yip G, Yu Y. 2012. Breast cancer metastasis. Cancer Genomics Proteomics. 9(5):311–320.

Selves J, Long-Mira E, Mathieu M-C, Rochaix P, Ilié M. 2018. Immunohistochemistry for diagnosis of metastatic carcinomas of unknown primary site. Cancers (Basel). 10(4):108. doi: 10.3390/cancers10040108

Shirke AA, Wang J, Ramamurthy G, Mahanty A, Walker E, Zhang L, Panigrahi A, Wang X, Basilion JP. 2024. Prostate specific membrane antigen expression in a syngeneic breast cancer mouse model. Mol Imaging Biol. 26(4):714–728. doi: 10.1007/s11307-024-01920-2

Silva WA Jr, Gnjatic S, Ritter E, Chua R, Cohen T, Hsu M, Jungbluth AA, Altorki NK, Chen Y-T, Old LJ, et al. 2007. PLAC1, a trophoblast-specific cell surface protein, is expressed in a range of human tumors and elicits spontaneous antibody responses. Cancer Immun. 7(1):18.

Stutterheim J, Gerritsen A, Zappeij-Kannegieter L, Kleijn I, Dee R, Hooft L, van Noesel MM, Bierings M, Berthold F, Versteeg R, et al. 2008. PHOX2B is a novel and specific marker for minimal residual disease testing in neuroblastoma. J Clin Oncol. 26(33):5443–5449. doi: 10.1200/JCO.2007.13.6531

Subkhankulova T, Gilchrist MJ, Livesey FJ. 2008. Modelling and measuring single cell RNA expression levels find considerable transcriptional differences among phenotypically identical cells. BMC Genomics. 9(1):268. doi: 10.1186/1471-2164-9-268

Tao K, Fang M, Alroy J, Sahagian GG. 2008. Imagable 4T1 model for the study of late stage breast cancer. BMC Cancer. 8(1):228. doi: 10.1186/1471-2407-8-228

Tarighati E, Keivan H, Mahani H. 2023. A review of prognostic and predictive biomarkers in breast cancer. Clin Exp Med. 23(1):1–16. doi: 10.1007/s10238-021-00781-1

Vandesompele J, De Preter K, Pattyn F, Poppe B, Van Roy N, De Paepe A, Speleman F. 2002. Accurate normalization of real-time quantitative RT-PCR data by geometric averaging of multiple internal control genes. Genome Biol. 3(7):RESEARCH0034. doi: 10.1186/gb-2002-3-7-research0034

Wang X, Baddoo MC, Yin Q. 2014. The placental specific gene, PLAC1, is induced by the Epstein-Barr virus and is expressed in human tumor cells. Virol J. 11(1):107. doi: 10.1186/1743-422X-11-107

Wang Z, Deng L, Xu X, Zhao L. 2023. Differential expression of PLAC1 and Netrin-1 in liver metastasis of colorectal cancer and its predictive value. BMC Gastroenterol. 23(1):275. doi: 10.1186/s12876-023-02908-y

Yu M, Bardia A, Wittner BS, Stott SL, Smas ME, Ting DT, Isakoff SJ, Ciciliano JC, Wells MN, Shah AM, et al. 2013. Circulating breast tumor cells exhibit dynamic changes in epithelial and mesenchymal composition. Science. 339(6119):580–584. doi: 10.1126/science.1228522

Zeraatkar N, Sajedi S, Kaviani S, Taheri M, Khanmohammadi H, Sarkar S, Ay MR. 2017. Development of a preclinical PET system based on pixelated LYSO crystals and SiPM arrays. In: 2017 IEEE Nuclear Science Symposium and Medical Imaging Conference (NSS/MIC). IEEE; p. 1–3.

Zhang J, Wei Q, Dong D, Ren L. 2021. The role of TPS, CA125, CA15-3 and CEA in prediction of distant metastasis of breast cancer. Clin Chim Acta. 523:19–25. doi: 10.1016/j.cca.2021.08.027

Zhao Q, He X, Qin X, Liu Y, Jiang H, Wang J, Wu S, Zhou R, Yu C, Liu S, et al. 2022. Enhanced therapeutic efficacy of combining losartan and chemo-immunotherapy for triple negative breast cancer. Front Immunol. 13:938439. doi: 10.3389/fimmu.2022.938439

Zhou Y, Tao L, Qiu J, Xu J, Yang X, Zhang Y, Tian X, Guan X, Cen X, Zhao Y. 2024. Tumor biomarkers for diagnosis, prognosis and targeted therapy. Signal Transduct Target Ther. 9(1):132. doi: 10.1038/s41392-024-01823-2

Zhu A, Lee D, Shim H. 2011. Metabolic positron emission tomography imaging in cancer detection and therapy response. In: Seminars in Oncology: 2011. Elsevier; p. 55–69.